논문 2001-10-1-09

Development of an Optical Waveguide Loss Measuring System using an Rectangular Glass Probe

Young-Kyu Choi

Abstract

The use of a glass-plate probe of rectangular shape is proposed for the measurement of transmission loss in optical waveguides. The light-collecting window is of a thin, rectangular shape and is perpendicular to the light streak, while the conventional fiberglass probe has a small circular face. This transversely elongated form results in a grate improvement of mechanical tolerance for the probe movement in the vertical as well as in the transverse direction. A theoretical investigation also presents a reasonable agreement with the experiments.

Key words : waveguide loss measurement, glass probe sensor

1. Introduction

There are two nondestructive methods to measure the transmission loss of optical planar waveguides[1]. One of them is known as the sliding-prism method[2, 3]. When a certain mode is supported on a slab waveguide, the mode power is coupled out to a prism that is slid along the light streak. Plotting the output power versus prism distance gives an exponential decay constant of the mode. Although this technique has the advantage that it is applicable even to a low-loss waveguide, it has the following disadvantages : (1) it is not easy to keep the output coupling constant as the prism slides because of the mechanical fluctuation in the course of the movement, and (2) frequent attachment and removal of the prism to and from the waveguide damages the waveguide as well as the prism itself.

Another method of loss measurement may be called the scattered-light detecting method[4-6]. Detection can be made either by a probe with a photodiode or by a camera (including a TV camera). Being a noncontacting detection, it is free from the disadvantages of (2) above. However, this method also has a disadvantage similar to (1) of the sliding-prism method, since a probe of optical fiber is used.

In this paper we have attempted to overcome these defects. Our proposal is to use a glass-plate probe instead of a fiberglass probe. In section 2 we consider the sensor probe and show the experimental setup. Mechanical tolerance of the sensor probe and the loss measuring results were described in section 3 and section 4, respectively. We analyze the proposed sensing system theoretically in section 5. And, we discussed the computed results comparing

신라대학교 광전자공학과
(Department of Photonics, Silla University)
<접수일자 : 2000년 10월 31일>

with the measured results in section 6.

2. Probe Consideration and Experimental Setup

Since a fiberglass probe has a small cross section, it is difficult for the probe to be controlled on the light streak both vertically and horizontally. In order to avoid the effect of horizontal fluctuation, a probe-scanning measurement has been analyzed and the maximum outputs have been plotted to obtain an exponential decay[1]. But this technique still suffers from the vertical fluctuation of the probe, and hence the improvement of the accuracy is limited in spite of the complication of the measurement system.

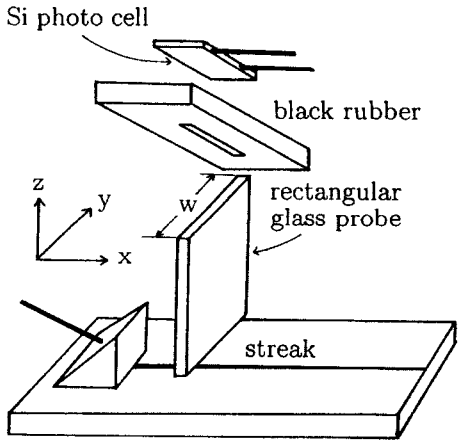

Fig. 1 Arrangement of the rectangular glass probe on a planar waveguide and the detector

We have therefore adopted a glass rod with a circular cross section since it forms a waveguide without cladding and has a wide collecting window, which may bring about better mechanical tolerance compared with that of a thin fiber probe. The thicker the probe is, the more stable the output becomes, versus the vertical or horizontal fluctuation of the probe. But we cannot make it too thick since the waveguide to be measured has a finite length, Thus we should limit the longitudinal dimension of the probe with the transverse dimension kept wide enough, which results in a rectangular probe with a Si photocell as the detector arranged as shown in Fig. 1. In this way, it is expected that the probe has both a relaxed tolerance of movement and a wide range of constant coupling strength.

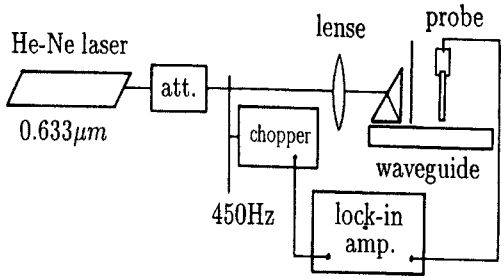

Fig. 2 Schematic diagram of the loss measuring system

Figure 2 is a block diagram of the measurement system.. A common Si photocell is wide enough to catch all the signals that come out from the probe. Any other type of glass may also be feasible for the probe, but only if it is transparent and has all the surfaces polished. The probe is mounted on an XYZ mechanical stage. Since the stray light degrades the S/N (signal-to-noise) ratio, a black absorber is painted on all the surfaces of the waveguide substrate, except the upper waveguide part. An automatic measurement, with the output plotted against the longitudinal movement of the probe, will be easily attained by using an XY recorder.

3. Mechanical Tolerance

3-1. Transverse Deviation

As the probe deviates transversely from the light streak (in the y direction in Fig. 1), the collected light at the window of the probe will decrease monotonically. But it will be almost constant as long as the deviation is less than half of the probe width. This expectation is demonstrated to be true in Fig. 3(a) by two experiments with rectangular probes of

different widths 4 mm and 10 mm with a 1 mm thickness. We used the same streak width in the two different measurements. The flatness of the output was satisfactory even for the narrower probe because the transverse probe deviation can easily be kept to less than 1 mm. The waveguide loss is as high as 10 dB/cm in this example. In Fig. 3(b) we also show a comparative experiment using a circular cylindrical probe.

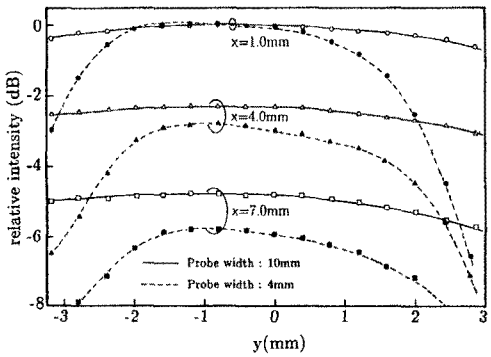

(a)

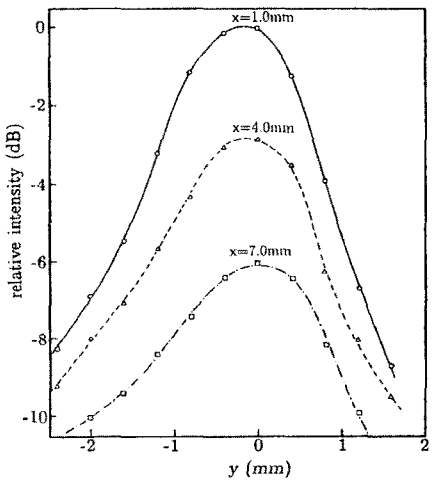

(b)

Fig. 3 Output intensity from the probe as a function of transverse deviation ($z=0.5$ mm).
(a) Rectangular probe(thickness 1 mm, waveguide loss dB/cm).
(b) Cylindrical probe(diameter 1.5 mm, *waveguide loss 10 dB/cm)*

This probe resembles a conventional fiberglass probe in the shape of its cross section, while it differs in that it is much thicker and has no cladding. In fact, the diameter of our probe is no less than 1.5 mm. Figure 3(b) tells us that a probe with a circular cross section is sensitive to the transverse deviation even if it is fairly thick. If it shifts transversely by 1 mm, the output decreases by more than 3 dB.

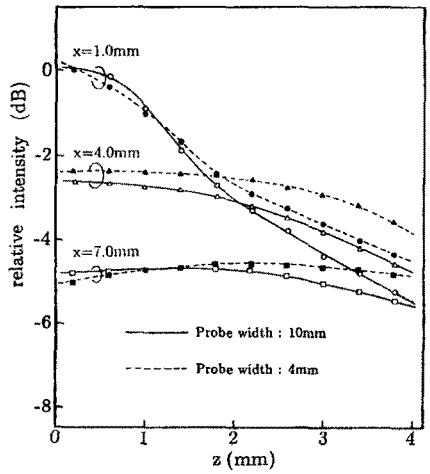

(a)

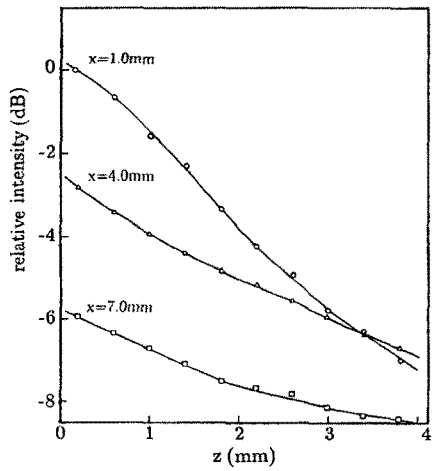

(b)

Fig. 4 Output intensity from the probe as a function of vertical deviation.
(a) Rectangular probe(thickness 1 mm, waveguide loss 10 dB/cm).
(b) Cylindrical probe (diameter 1.5 mm, waveguide loss 10dB/cm).

3-2. Vertical Deviation

The detecting probe also fluctuates vertically (in the z direction in Fig. 1). The output variation against the probe height is plotted in Fig, 4(a). We used the same rectangular probe that is used in measuring the transverse deviation. It may seem strange that the output increases with height at a long distance from the input prism, but this characteristic can be explained as follows.

Let us consider the limiting case where the waveguide is without loss and hence the intensity of the light streak is constant. If the probe were infinitely wide in the $y$direction, the incident flux into the probe would not change with the probe height. This means that a wide rectangular probe will be highly insensitive to the vertical fluctuation if the waveguide loss is small. On the other hand, if the waveguide loss is large as in the case of Fig. 4, the streak is stronger at smaller x. Therefore, the probe collects more flux when it goes upward, because the stronger light from the source (more to the left) enters the probe with a smaller incident angle. Figure 4 illustrates the vertical tolerance of a circular cylindrical probe. This is a well-behaved example for a probe with a circular cross section since it is much thicker than a conventional fiber probe.

4. Loss Measurement

We have constructed an automatic measurement system, as mentioned in Section 2. The input to the x axis of a recorder is provided by a potentiometer connected to the rotary shaft of an optical XYZ stage. The lowest TE mode was excited by a rutile prism in the optical waveguide being tested. Attenuation constants are estimated from the slope of the straight (it is hoped) lines drawn by an XY recorder. We show some of the results in Fig. 5. Figure 5(a) is for an Nb_2O_5 Corning 7059 glass structure.

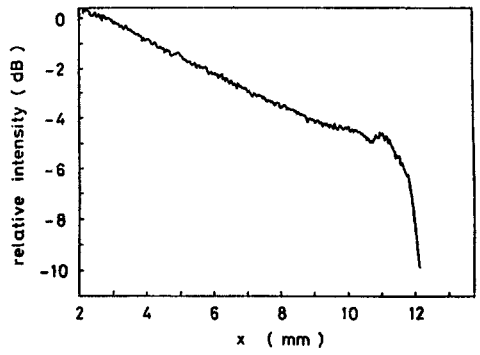

(a)

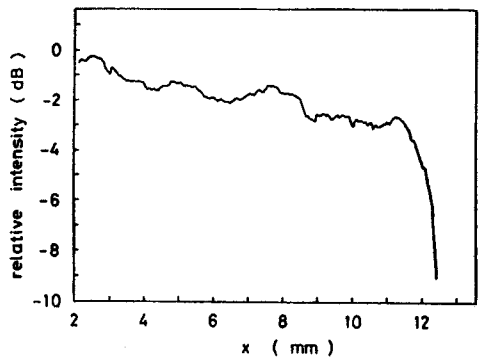

(b)

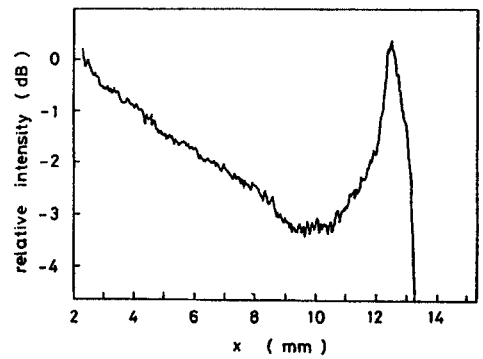

(c)

Fig. 5 Three examples of automated loss measurement.
(a) Nb_2O_5 Corning 7059 waveguide,
(b) Nb_2O_5-$LiTaO_3$ waveguide,
(c) Nb-diffused $LiTaO_3$ waveguide

A Nb_2O_5 amorphous film was fabricated by a RF magnetron sputtering apparatus in Ar : 80% - O_2 : 20% atmosphere with a water-cooled substrate. The refractive indices of the film and the substrate were

2.25 and 1.53, respectively, and the film thickness was 0.3 ㎛. Since the film was so thin, the attenuation constant was calculated to be as high as 6.9 dB/cm. The light streak was uniform and of high intensity indicating that the attenuation came mainly from the surface scattering. The second example is shown n Fig. 5(b), which is for a Nb_2O_5-$LiTaO_3$ structure. The Nb_2O_5 film was fabricated in the same way as the film in Fig. 5(a). Although this waveguide had a smaller loss (3.0 dB/cm), the streak was less nearly uniform because of many randomly located scattering points. It corresponds to type (b) of the three categories of Gottlieb's paper[4]. The third waveguide was created by Nb the waveguide was not painted black in this case. The attenuation constant was fairly large, which means that the loss mechanism was mainly absorption in the guide, or that most of the scattered light went downward and was absorbed by the black paint at the bottom.

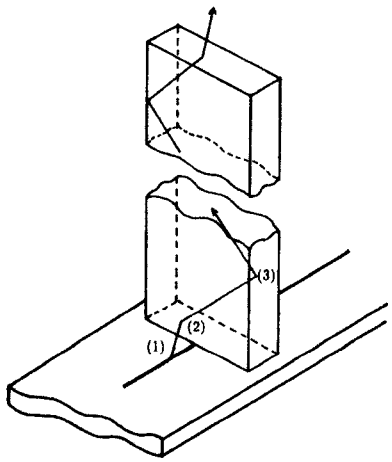

Fig. 6 Three difficulties in formulating the output of a rectangular probe.

5. Theoretical Consideration

There are many obstacles that hinder the formulation of the problem. These are illustrated in Fig. 6 and are explained below in the order given in the illustration. (1) It is not known how much light reaches the probe, because the directivity (radiation pattern) of the scattered light from a streak differs from waveguide to waveguide[7-9]. (2) The transmission coefficient in the probe is different according to the polarization of incident light, and it depends on what mode is excited[10-11]. (3) The light caught in the probe goes upward, repeating total reflection at the side walls of the probe. Since the polarizations change at the each reflection, the ratio of the *p* and *s* polarizations of the output light varies with the reflection angle at each wall[12, 13]. This results in a change of the photocell output.

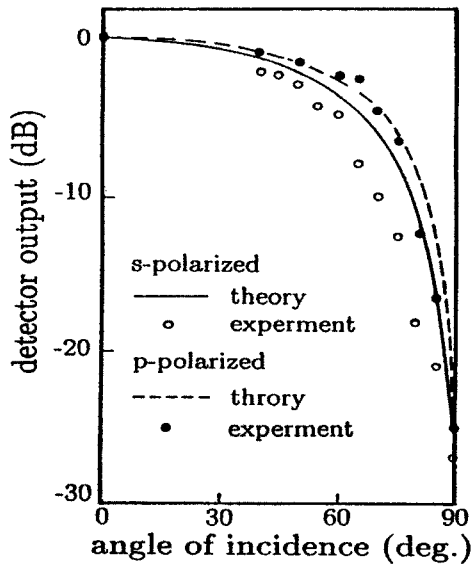

Fig. 7 Detector output as a function of the incident angle of the collimated beam.

A formulation that takes into account the above-mentioned points is not impossible, but unnecessarily complicated. Thus, we will make a simplified theoretical estimation with the following assumptions. (1) The radiation pattern from the light streak is a cosine function of the polar angle, which takes a maximum value at a scattered light from the light streak is equally distributed in *p* and *s* directions (no polarization), and (3) all the energy entering into the probe is detected by the photo-cell. Before we performed the numerical calculation of

Eq.(8), we examined experimentally the response of the detecting system composed of the probe and the photo-cell, so as to confirm the validity of assumption (3).

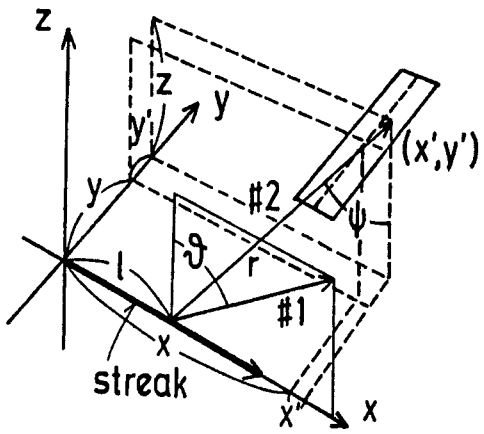

Fig. 8 Coordinate system for calculating the flux incident into the end face of the probe.

The incident-angle dependence is shown in Fig. 7, indicating a close agreement with the theory.

The detected signal power may be proportional to the product of $\cos\psi$ and the transmission coefficient T_P or T_S at the air-glass interface, where ψ denotes the incident angle at the probe end face ; n_g is the refractive index of probe glass, and

$$T_P = 1 - \frac{\tan(\psi - \psi')}{\tan(\psi + \psi')},$$

$$T_S = 1 - \frac{\sin(\psi - \psi')}{\sin(\psi + \psi')}, \qquad (1)$$

$$\psi' = \sin^{-1}\left(\frac{1}{n_g}\sin\psi\right).$$

Figure 8 shows the coordinate system and the probe configuration. We drew line #1, which passes through point $(l, 0, 0)$ on the streak, making an angle θ with the z axis in the $x-z$ plane (incident plane). Line #1 was set for the sake of easier calculation, so that the angle θ can be chosen arbitrarily. The direction cosine of line #1 is $(\sin\theta, 0, \cos\theta)$. We introduce another coordinate system (x', y') for the infinitesimal element $dx'dy'$ on the probe end face. The line between this element and point $(l, 0, 0)$ is denoted as #2, the direction cosine (α, β, γ) being given by

$$\alpha = \frac{x + x' - l}{r}, \quad \beta = \frac{y + y'}{r}, \quad \gamma = \frac{z}{r} \qquad (2)$$

where

$$r = [(x + x' - l)^2 + (y + y')^2 + z^2]^{1/2} \qquad (3)$$

Here we introduce χ for the angle between lines #1 and #2 so that we obtain relation

$$\cos\chi = \alpha\sin\theta + \gamma\cos\theta \qquad (4)$$

Substituting Eqs.(2) and (3) into Eq.(4) yields

$$\cos\chi = \frac{(x + x' - l)\sin\theta + z\cos\theta}{[(x + x' - l)^2 + (y + y')^2 + z^2]^{1/2}} \qquad (5)$$

The flux incident to the element $dx'dy'$ from the source Idl at $(l, 0, 0)$ is written as

$$dP' \propto Idl\frac{dx'dy'\cos\psi}{r^2}\cos\chi \qquad (6)$$

where the second term on the right-hand side is of Eq.(6) the solid angle spanning the element $dx'dy'$ from the source at $(l, 0, 0)$. The angle ψ between line #2 and the z direction obviously satisfies the relation

$$\cos\psi = \frac{z}{r} = \frac{z}{[(x + x' - l)^2 + (y + y')^2 + z^2]^{1/2}} \qquad (7)$$

Now, we can integrate relation (6) to get the total flux

$$P \propto \int_{-w/2}^{w/2} \int_{-t/2}^{t/2} \int_{0}^{\infty} \frac{I_o e^{-\alpha l} \cos\psi \cos\chi \, T}{r^2} \, dl \, dx' dy' \qquad (8)$$

where α denotes the attenuation constant of the waveguides, w and t are the width and thickness, respectively, of the rectangular probe, and the averaged transmission coefficient T is given by

$$T = \frac{T_P + T_S}{2} \qquad (9)$$

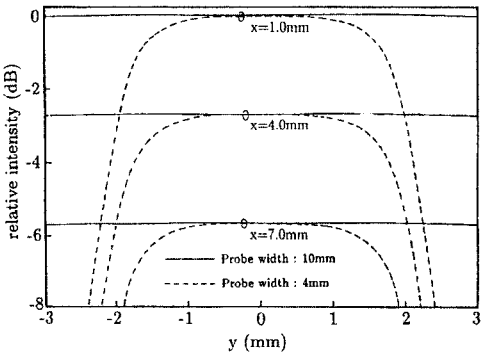

(a)

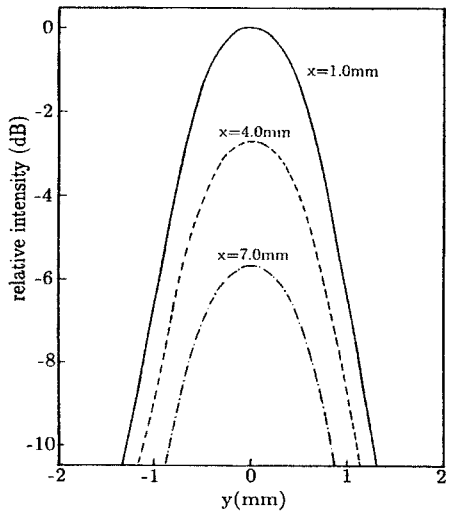

(b)

Fig. 9 Theoretical output intensity from the probe as a function of transverse deviation ($z = 0.5$ mm), (a) Rectangular probe(thickness 1 mm, waveguide loss 10 dB/cm), (b) Cylindrical probe (diameter 1.5 mm, waveguide loss 10 dB/cm).

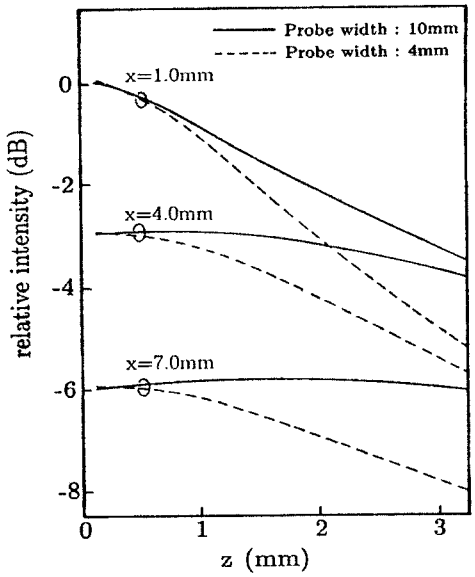

(a)

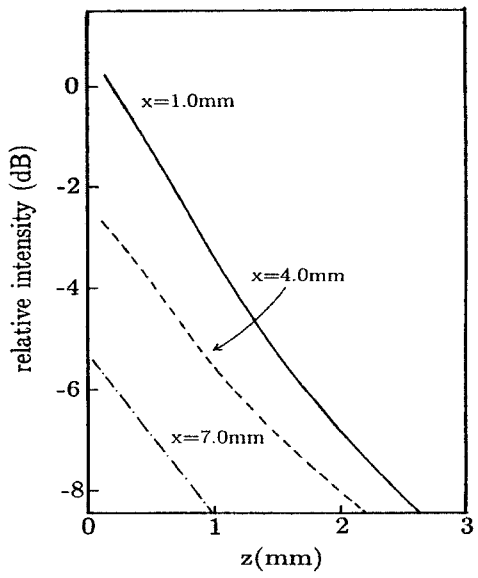

(b)

Fig. 10 Theoretical output intensity from the probe as a function of vertical deviation, (a) Rectangular probe(thickness 1 mm, waveguide loss 10 dB/cm), (b) Cylindrical probe (diameter 1.5 mm, waveguide loss 10 dB/cm).

6. Computed Results and Dicussions

The triple integral of relation (8) gives the

calculated mechanical tolerance in Figs. 9 and 10. The parameters were chosen to be the same as in Figs. 3 and 4, respectively. The angle of directivity θ was taken to be 0° for simplicity. They are qualitatively in good agreement. In fact, examining the z dependence of the output of Fig. 10(a), we notice that the output increases with small z when w is large, while it decreases with z when w is small. This feature agrees with the experimental result shown in Fig. 4(a).

Figures 9(b) and 10(b) are for a circular cylindrical probe, corresponding to Figs. 3(b) and 4(b). The experimental and theoretical results also agree well in this case.

7. Conclusions

For the scattered-light probing method extensively employed for planar-waveguide loss measurement, we have proposed to use a rectangular glass probe instead of a conventional fiberglass probe. Our probe means a conversion from a one-dimensional end face to a two-dimensional end face, since the cross section of a fiberglass probe is like a line. Our new probe resulted in a significant improvement of the mechanical tolerance of probe movement as well as an increase of the detecting signal. Although we had done experiments that used the high-loss waneguide (10 dB/cm) at this time, considering the physical stability of the wide probe cross section this technique can apply to low-loss measurements, that is, below 1 dB/cm. These characteristics have made it easier to automatize the measurement, and the time for measurement has been reduced considerably.

Acknowledgements

This study was supported in part by research funds from Silla University, 2000.

References

1. J. E. Goell and R. D. Standly, " Sputtering glass waveguide for integrated optica circuits", Bell Syst. Tech., J. Briefs 48, 3345-3346, 1969.
2. P. K. Tien and R. Ulrich, " Theory of prism-film coupler and thin-film light guides," J. Opt. Soc. Am., 60 no.70, p. 1325, Oct. 1970.
3. H. P. Weber, F. A. Dumn and W. N. Leibolt, "Loss measurements in thin film optical waveguides," Appl. Opt. Vol. 12, no. 4 p 755, April, 1973.
4. M. Gottlieb, G. B. Brandt, and J. J. Conroy, " Out of-plane sacttering in optical waveguides," IEEE Trans. Circuits Syst. CAS-26, 1029-1035, 1979.
5. M. Imai, Y. Ohtsuka and M. Koseki, "Scattering pattern measurement and analysis of sputtered-glass optical waveguides for integrated optics," IEEE. J. Quantum Electron, QE-18, No. 4 p. 789, April, 1982.
6. D. G. Hall, "In-plane scattering in planar optical waveguides, refractive-index fluctutions and surface roughness," J. Opt. Soc. Am. A, vol. 2, no. 5, pp. 747-752, 1985.
7. Y. Suematsu and K. Furuya, " Characteristic mode and scattering loss of asymmetric slab optical waveguides." Electron. Commun. Jpn. 56-C, 277-284, 1973.
8. S. Miyanaga, M. Imai, and T. Asakura, " Radiation pattern of light scattering from the core region of dielectric-slab-optical waveguides," IEEE J. Quantum Electron. QE-14, 30-37, 1978.
9. Y. Suematsu, K. Furuya, M. Hakuta, and K. Chiba, "Far field radiation pattern caused by random wall distribution of dielectric waveguides and determination of correlation length," Electron. Commun. Jpn. 56-C, 377-384, 1973.
10. D. Marcuse "Radiation losses of dielectric

waveguides in terms of the power spectrum of the wall distortion function", Bell System Tech. J. vol. 48, p 3233, Dec, 1969.

11. D. Marcuse, "Power Distribution and radiation losses in multimode dielectric slab waveguides," Bell System Tech. J. vol. 51, p429, Feb. 1972.
12. T. Tarmir, Guided-wave Optoelectronics, Springer-Verlag, New York, 2nd ed, 1990.
13. H. Nishihara, M. Haruna and T. Suhara, Optical Integrated Circuits, McGraw-Hill, New York, 1989.

著 者 紹 介

Young-Kyu Choi received his M. S. and Ph. D degree from Kyoto University, Kyoto, Japan. in 1989 and 1992, respectively. From 1992 to 1995, he was a full-time lecturer of Fukui University, Fukui, Japan. He is now a professor in the Department of Photonics, Silla University, Pusan, Korea. His research interests include the ultra-high-speed optical modulator and demodulator, optical waveguide design and analysis, optical signal processing, microwave photonics and millimeterwave antenna. He is presently a member of the IEICE, PPAP, OSA and IEEE.